

**MATHEMATICAL MODELLING OF PULSATILE HERSCHEL BULKLEY FLUID FLOW THROUGH AN INCLINED STENOSED ARTERY WITH BODY ACCELERATION & SLIP**

**S. U. SIDDIQUI, CHHAMA AWASTHI\***

**Department of Mathematics,  
Harcourt Butler Technical University, Kanpur-208002, Uttar Pradesh, India.**

*(Received On: 08-06-17; Revised & Accepted On: 14-07-17)*

---

**ABSTRACT**

*In this study, a mathematical model has been developed to investigate the effect of body acceleration and slip in the pulsatile flow of Herschel Bulkley fluid through an inclined stenosed artery. A Perturbation method is used to solve the system of non linear differential equations with suitable boundary conditions. The analytical expressions for axial velocity, flow rate, wall shear stress and effective viscosity has been derived with the help of MATLAB. The combined effect of body acceleration, slip and inclination has been seen and it has been observed that the axial velocity and flow rate increases with the increase in body acceleration, inclination angle, pressure gradient and slip velocity while decreases with the increase in yield stress and stenosis height. As time increases, wall shear stress gradually decreases and attains symmetry. Effective viscosity decreases with body acceleration and slip. The present study also brings out the effects of asymmetric of the stenosis on the flow characteristics.*

**Keywords:** *Stenosis; Blood; Pulsatile flow; Herschel Bulkley Fluid; Slip velocity; Body acceleration.*

---

**1. INTRODUCTION:**

In human physiology, the theoretical analysis on blood flow through the obstructed artery is very useful as it plays a vital role to diagnose and understand many cardiovascular diseases such as coronary thrombosis, angina, strokes etc. The reason behind the malfunction of cardio-vascular system is an impediment developed inside the lumen of an artery. This hindrance in the artery is due to the presence of atherosclerosis. Among the various arterial diseases, Atherosclerosis (stenosis) is the common disease which is caused by the invasion and deposition of lipoproteins, fats, cholesterol at the sites of atherosclerotic lesion in the artery.

In our daily life, several times we experiences the body acceleration while sudden movement of body parts during sports activity, fast driving, travelling in vehicle etc. Due to this body acceleration, different health hazards arises such as headache, increase in pulse rate etc. Tu and Deville [1] observed that the blood in diseased conditions, for instance, patients with severe cerebrovascular diseases exhibits power law behaviour. Pulsatile flow of blood through a rigid circular tube subjected to periodic body acceleration considering blood as Newtonian fluid is presented by Sud and Sekhon [27]. The pulsatile flow of Casson's fluid with body acceleration subject to a slip velocity condition in stenosed artery is studied by Siddiqui *et al.* [26]. Young and Liepsch [6, 10] compared the details of flow behaviors with hemodynamic approach and observed that during a flow cycle, flow rate varies over a wide range due to pulsatile nature of blood. Biswas and Kapur [3, 15] studied the non-Newtonian fluid models and stated that Casson and Herschel bulkley fluid can be widely used in fundamental understanding of blood flow phenomena. Generally, blood flow in narrow arteries is assumed as Pulsatile and it has been observed that physiological conditions are probably related to pulsatile model. Blood is pulsatile as heart pumps the blood is periodic in nature. D.S Shankar and K. Hemlata [9] have described the effects of pulsatility, stenosis and non-Newtonian behavior of blood, assuming blood to be Herschel Bulkley fluid. D.S Shankar and Lee [8] studied these dynamic behaviors of blood with axially symmetric stenosis and asymmetric stenosis. Chaturani and Ponnalagar Samy [21] have mentioned that blood behaves like Herschel-Bulkley fluid rather than Power law and Bingham fluids for tube diameter 0.095 mm. The velocity profile in the arterioles having diameter less than 0.1 mm are generally explained fairly by Casson and Herschel-Bulkley fluid models is analyzed by Iida [19]. An effect of slip in blood flow through stenosed tube is analyzed by Chaturani and Biswas [20]. Effects of stenosis shape parameter and slip on various flow parameters, considering blood as Bingham Plastic fluid with axially non-symmetric stenosed artery is developed by Shah [25]. Young, Liu and Chakravarty *et al.* [5, 12, 23] analyzed the pulsatility of blood by treating blood as a Newtonian fluid. Mishra *et al.* and Ookwara *et al.* [14, 24] observed that blood being suspension of corpuscles in plasma behaves like a non-Newtonian fluid when it flows through larger arteries at high shear rate while it can be assumed as Newtonian when it passes through narrow arteries (0.02-0.1mm) at low shear rate ( $< 10/s$ ) particularly in diseased state[7].

It can be seen easily that in physiological systems all arteries are not horizontal; few of them are inclined, therefore a gravitational force has been accounted there due to inclination. Maruti Prasad and Radha Krishnamcharya [16] have proposed a model of steady blood flow through an inclined artery with a stenotic wall. Biswas and Paul [3] proposed a mathematical model on the steady flow of blood through an inclined tapered constricted artery assuming blood as Newtonian fluid, with an axial slip velocity at the vessel wall. The peristaltic transport of Herschel Bulkley fluid through an inclined tube is discussed by Vajravelu *et al.* [17]. Chaturani and Upadhyaya [22] investigated the gravityflow of fluid with couple stress along an inclined plane. Sanyal *et al.* [4] discussed the characteristics of blood flow by assuming blood to be couple stress fluid in a rigid inclined circular tube with periodic body acceleration under the influence of a uniform magnetic field. Pulsatile flow of blood in a catheterized inclined artery with a slip velocity at the stenosed arterial wall under the influence of magnetic field is discussed by the Sharma *et al.* [18]. With the above motivations, present investigation has been established to analyze the effect of body acceleration, slip velocity, stenosis shape parameter and inclined angle on arterial flow characteristics by considering the blood as Herschel bulkley fluid. The effect of pulsatility and asymmetric shape of the stenosis on the flow parameters has been also studied which could be helpful to further understand the behavior of different fluid flow characteristics in the development and progression of arterial diseases.

## 2. MATHEMATICAL FORMULATION

Consider an axially symmetric, laminar, pulsatile and fully developed blood flow in an inclined arterial segment having axially non- symmetric stenosis but in radially symmetric manner and stenosis is depend upon the axial distance 'z'. The blood is modeled as a Herschel bulkley fluid in the presence of externally imposed periodic body acceleration and slip. It is assumed that the pulsatile flow in the artery is due to a prescribed periodic pressure gradient. We have used cylindrical polar co-ordinates  $(\bar{r}, \bar{\phi}, \bar{z})$ , where  $\bar{r}$  and  $\bar{z}$  denote the radial and axial co-ordinates. The mathematical expression for the radius of the artery Fig.1 can be written as [7]

$$\left. \begin{aligned} \frac{\bar{R}(\bar{z})}{\bar{R}_0} &= 1 - \bar{\xi} \left[ \bar{L}_s^{(m-1)} (\bar{z} - \bar{d}) - (\bar{z} - \bar{d})^m \right], \bar{d} \leq \bar{z} \leq \bar{d} + \bar{L}_s \\ &= 1, \quad \text{otherwise} \end{aligned} \right\} \quad (1)$$

Where  $\bar{R}(\bar{z})$  and  $\bar{R}_0$  is the radius of the artery with and without stenosis respectively,  $\bar{d}$  is the location of the stenosis,  $\bar{L}_s$  is the length of the stenosis and  $m \geq 2$  is the stenosis shape parameter and when  $m = 2$  stenosis becomes radially symmetric. Where the parameter  $\bar{\xi}$  is given by

$$\bar{\xi} = \frac{\bar{\delta}}{\bar{R}_0 \bar{L}_s^m} \frac{m^{m/(m-1)}}{(m-1)}$$

Where  $\bar{\delta}$  denotes the maximum height of the stenosis at  $\bar{z} = \bar{d} + \bar{L}_s / m^{1/(m-1)}$  such that  $\bar{\delta} / \bar{R}_0 \ll 1$ .

The periodic body acceleration  $\bar{B}(\bar{t})$  in the axial direction is given by

$$\bar{B}(\bar{t}) = a_0 \cos(\bar{\omega}_b \bar{t} + \phi) \quad (2)$$

Where  $a_0$  is the amplitude and  $\phi$  is the phase angle of body acceleration with respect to the pressure gradient.  $\bar{\omega}_b = 2\pi \bar{f}_b$ ;  $\bar{f}_b$  is its frequency in Hz. The frequency of the body acceleration  $\bar{f}_b$  is assumed to be small so that wave effect can be neglected.

Since the pressure gradient is the function of  $\bar{z}$  and  $\bar{t}$ , therefore can be represented as

$$\frac{-\partial \bar{p}}{\partial \bar{z}}(\bar{z}, \bar{t}) = A_0 + A_1 \cos(\bar{\omega}_p \bar{t}), \quad t \geq 0 \quad (3)$$

Where  $A_0$  is the steady state pressure gradient,  $A_1$  is the amplitude of the fluctuating component and both  $A_0, A_1$  are function of  $\bar{z}$ . It can be seen that the radial velocity is very small in magnitude so that it may be neglected for problem with mild stenosis. The frequency of oscillation of the pulsatile flow is denoted by  $\bar{\omega}_p$  and defined as  $\bar{\omega}_p = 2\pi \bar{f}_p$ , where  $\bar{f}_p$  is the pulse rate frequency.

The basic momentum equations governing the fluid flow are given by Schlichting and Gersten [12].

$$\bar{\rho}(\partial\bar{v}/\partial\bar{t}) = -(\partial\bar{p}/\partial\bar{z}) - (1/\bar{r}) \frac{\partial}{\partial\bar{r}}(\bar{r}\bar{\tau}) + \bar{B}(\bar{t}) + \bar{\rho}g \sin\psi \quad (4)$$

$$\partial\bar{p}/\partial\bar{r} = 0 \quad (5)$$

Where  $\bar{v}$  represents the axial velocity along  $\bar{z}$  direction,  $\bar{t}$  is the time,  $\bar{\rho}$  is the density,  $\bar{p}$  is the pressure,  $\bar{\tau}$  is the shear stress,  $\psi$  is the inclination angle and  $\bar{B}(\bar{t})$  is the body acceleration, mathematically this body acceleration is described in equation (2).

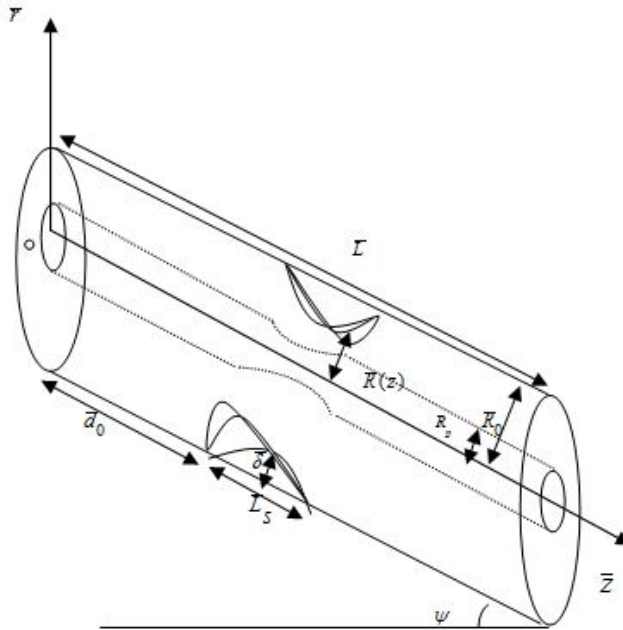


Fig. 1 Geometry of an axially non-symmetrical inclined stenosed artery

The constitutive equation in one dimensional form for Herschel Bulkley fluid is expressed as

$$\left. \begin{aligned} \bar{\tau} &= \bar{\tau}_y + \bar{\mu}_y^{1/n} (-\partial\bar{v}/\partial\bar{r})^{1/n} ; \text{if } \bar{\tau} \geq \bar{\tau}_y \\ \partial\bar{v}/\partial\bar{r} &= 0 ; \text{if } \bar{\tau} < \bar{\tau}_y \end{aligned} \right\} \quad (6)$$

Where  $\bar{\tau}_y$  denotes yield stress and  $\bar{\mu}_y$  denotes the coefficient of viscosity for Herschel Bulkley fluid with the dimension  $(ML^{-1}T^{-2})^n T$  and  $n$  is the flow behavior index of blood. In the core region where the shear stress is less than the yield stress (i.e.  $\bar{\tau} < \bar{\tau}_y$ ), the velocity gradient vanishes and this shows the plug flow. However the fluid behavior is indicated in the region  $\bar{\tau} > \bar{\tau}_y$ .

## 2.1 BOUNDARY CONDITIONS

The boundary conditions are

$$\bar{v} = \bar{v}_s \text{ at } \bar{r} = \bar{R}(\bar{z}) \quad (7)$$

$$\bar{\tau} \text{ is finite at } \bar{r} = 0 \quad (8)$$

Where  $\bar{v}_s$  is the axial slip velocity at the stenotic wall.

Let us introduce the following non-dimensional variables

$$\left. \begin{aligned} v &= \frac{\bar{v}}{A_0 \bar{R}_0^2 / 4 \bar{\mu}_0}, z = \bar{z} / \bar{R}_0, R(z) = \bar{R}(\bar{z}) / \bar{R}_0, r = \bar{r} / \bar{R}_0, d = \bar{d} / \bar{R}_0, L_s = \bar{L}_s / \bar{R}_0, t = \bar{t} \bar{\omega}_p, \\ F &= A_0 / 4 \bar{\rho} g, \omega = \bar{\omega}_b / \bar{\omega}_p, \delta = \bar{\delta} / \bar{R}_0, v_s = \frac{\bar{v}_s}{A_s \bar{R}_0^2 / 4 \bar{\mu}_0}, \tau = \frac{\bar{\tau}}{A_0 \bar{R}_0 / 2}, \alpha^2 = \frac{\bar{R}_0^2 \bar{\omega}_p \bar{\rho}}{\bar{\mu}_0}, \\ \xi &= \bar{\xi} / \bar{R}_0^{1-m}, e = A_1 / A_0, B = a_0 / A_0, \tau_y = \frac{\bar{\tau}_y}{A_0 \bar{R}_0 / 2}, \bar{\mu}_0 = \bar{\mu}_y \left[ \frac{2}{A_0 \bar{R}_0} \right]^{n-1} \end{aligned} \right\} \quad (9)$$

Where  $\alpha$  is the pulsatile Reynold's number or generalized Womersley frequency parameter.

Using non-dimensional variables, equation (4) becomes

$$\alpha^2 \left( \frac{\partial v}{\partial t} \right) = 4(1 + e \cos t) + 4B \cos(\omega t + \phi) - \left( \frac{2}{r} \right) \frac{\partial}{\partial r} (r\tau) + \frac{\sin \psi}{F} \quad (10)$$

Equation. (6) becomes

$$\begin{aligned} \tau &= \tau_y + \left( \frac{1}{2} \frac{\partial v}{\partial r} \right)^{1/n} \quad ; \text{if } \tau \geq \tau_y \\ \frac{\partial v}{\partial r} &= 0 \quad ; \text{if } \tau < \tau_y \end{aligned} \quad (11)$$

The boundary conditions (7) and (8) reduces to

$$v = v_s \text{ at } r = R(z) \quad (12)$$

$$\tau \text{ is finite at } r = 0 \quad (13)$$

The geometry of an arterial stenosis in non-dimensional form is given by

$$R(z) = \begin{cases} 1 - \xi \left[ L_s^{m-1} (z-d) - (z-d)^m \right], & d \leq z \leq d + L_s \\ 1, & \text{otherwise} \end{cases} \quad (14)$$

The non-dimensional volumetric flow rate is defined by

$$Q(z, t) = 4 \int_0^{R(z)} r v(z, r, t) dr \quad (15)$$

Where  $Q(z, t) = \frac{\bar{Q}(\bar{z}, \bar{t})}{\pi A_0 (\bar{R}_0)^4 / 8 \bar{\mu}_0}$ ;  $\bar{Q}(\bar{z}, \bar{t})$  is the volumetric flow rate.

Effective viscosity  $\bar{\mu}_e$  defined as

$$\bar{\mu}_e = \pi \left( - \frac{\partial \bar{p}}{\partial \bar{z}} \right) (\bar{R}(\bar{z}))^4 / \bar{Q}(\bar{z}, \bar{t})$$

Can be expressed in the non dimensional form as

$$\mu_e = R^4 (1 + e \cos t) / Q(z, t) \quad (16)$$

### 3. ANALYSIS OF THE PROBLEM

In this paper perturbation method is used and on using this method, the assumed form of the solution reflects the physical principle which states that the inertial effects are not significant for smaller values of frequency parameter which determines the pressure gradient. Since non-dimensionalize equation (10), (11) has  $\alpha^2$  term which is dependent on time, therefore expanding equation (10), (11) about  $\alpha^2$ . The axial velocity  $v$ , shear stress  $\tau$ , plug core radius  $R_p$ , plug core velocity  $v_p$  and plug core shear stress  $\tau_p$  are expressed as follows in terms of  $\alpha^2$  (where  $\alpha^2 \ll 0$ ).

$$v(z, r, t) = v_0(z, r, t) + \alpha^2 v_1(z, r, t) + \dots \tag{17}$$

$$\tau(z, r, t) = \tau_0(z, r, t) + \alpha^2 \tau_1(z, r, t) + \dots \tag{18}$$

$$R_p(z, t) = R_{0p}(z, t) + \alpha^2 R_{1p}(z, t) + \dots \tag{19}$$

$$v_p(z, t) = v_{0p}(z, t) + \alpha^2 v_{1p}(z, t) + \dots \tag{20}$$

$$\tau_p(z, t) = \tau_{0p}(z, t) + \alpha^2 \tau_{1p}(z, t) + \dots \tag{21}$$

Substituting equation (17) and (18) in equation (10) and equating the constant term and  $\alpha^2$  term, we get

$$\frac{\partial}{\partial r}(r\tau_0) = 2r \left[ (1+e \cos t) + B \cos(\omega t + \phi) + \frac{\sin \psi}{4F} \right], \tag{22}$$

$$\frac{\partial v_0}{\partial t} = -\frac{2}{r} \frac{\partial}{\partial r}(r\tau_1) \tag{23}$$

Integrating equation (22) between 0 and  $R_{0p}$  and using boundary condition (13), we get

$$\tau_{0p} = R_{0p} a(t) \tag{24}$$

$$\text{Where } a(t) = [(1 + e \cos t) + B \cos(\omega t + \phi) + \frac{\sin \psi}{4F}]$$

Integrating equation (22) between  $R_{0p}$  and  $r$  and with the use of equation (24), we get

$$\tau_0 = r a(t) \tag{25}$$

Substituting equation (17) and (18) in equation (11), we get

$$-\frac{\partial v_0}{\partial r} = 2 \tau_0^{n-1} [\tau_0 - n \tau_y] \tag{26}$$

$$-\frac{\partial v_1}{\partial r} = 2 n \tau_0^{n-2} [\tau_0 - (n-1) \tau_y] \tag{27}$$

Integrating equation (26) between  $r$  and  $R$ , with the help of equation (25) and (12), we obtain

$$v_0 = v_s - 2 \tau_y \int_0^r [a(t)]^{n-1} (R^n - r^n) + \frac{2[a(t)]^n}{(n+1)} (R^{n+1} - r^{n+1}) \tag{28}$$

From equation (28), plug core velocity  $v_{0p}$  can be obtained as

$$v_{0p} = v_s - 2 \tau_y [a(t)]^{n-1} (R^n - R_{0p}^n) + \frac{2[a(t)]^n}{(n+1)} (R^{n+1} - R_{0p}^{n+1}) \tag{29}$$

Neglecting the terms with  $\alpha^2$  and higher powers of  $\alpha$  in equation (19), with the help of equation (24),  $R_{0p}$  can be obtained as

$$r|_{\tau_{0p}=\tau_y} = R_{0p} = \frac{\tau_y}{a(t)} \tag{30}$$

Similarly solving equation (23) with the help of equation (28), (29) and boundary condition (12), (13) we get the solutions for  $\tau_1, \tau_{1p}$  as

$$\tau_1 = a_5 r - a_4 r^{n+1} + a_6 r^{n+2} \tag{31}$$

$$\tau_{1p} = a'_5 R_{0p} - a'_4 R_{0p}^{n+1} + a'_6 R_{0p}^{n+2} \tag{32}$$

Where

$$a_1 = [a(t)]^{n-2} a'(t), \quad a_2 = na(t)a_1(t)R^{n+1}/2(n+1), \quad a_3 = (n-1) \tau_y a_1(t) R^n / 2, \quad a_4 = (n-1) \tau_y a_1(t) / (n+2),$$

$$a_5 = a_3 - a_2, \quad a_6 = na(t)a_1(t) / (n+1)(n+3), \quad a'_4 = (n-1) \tau_y a_1(t) / 2, \quad a'_5 = -(a_2 - a_3), \quad a'_6 = na(t)a_1(t) / 2(n+1)$$

From equation (27) with the help of equation (25), (31), axial velocity  $v_1$ , Plug core velocity  $v_{1p}$  can be obtained as

$$v_1 = 2b_2 (R^n - r^n) - b_3 (R^{2n} - r^{2n}) + b_4 (R^{2n+1} - r^{2n+1}) + 2b_6 (R^{n+1} - r^{n+1}) - 2b_7 (R^{2n+1} - r^{2n+1}) + b_8 (R^{2n+2} - r^{2n+2}) \quad (33)$$

$$v_{1p} = 2b_2 (R^n - R_{0p}^n) - b_3 (R^{2n} - R_{0p}^{2n}) + b_4 (R^{2n+1} - R_{0p}^{2n+1}) + 2b_6 (R^{n+1} - R_{0p}^{n+1}) - 2b_7 (R^{2n+1} - R_{0p}^{2n+1}) + b_8 (R^{2n+2} - R_{0p}^{2n+2}) \quad (34)$$

Where

$$b_1 = [a(t)]^{n-2} \tau_y, b_2 = (1-n)a_5 b_1, b_3 = (1-n)a_4 b_1, b_4 = 2n(1-n)a_6 b_1 / (2n+1), b_5 = n[a(t)]$$

$$b_6 = a_5 b_5 / (n+1), b_7 = a_4 b_5 / (2n+1)$$

With the help of equation (28), (29) and (33), (34) in (17) and (20), the axial velocity  $v$ , plug core velocity  $v_p$  can be obtained as

$$v = v_f - 2 \tau_y [a(t)]^{n-1} (R^n - r^n) + \frac{2[a(t)]^n}{(n+1)} (R^{n+1} - r^{n+1}) + \alpha^2 \left[ \begin{array}{l} 2b_2 (R^n - r^n) - b_3 (R^{2n} - r^{2n}) \\ + b_4 (R^{2n+1} - r^{2n+1}) + 2b_6 (R^{n+1} - r^{n+1}) \\ - 2b_7 (R^{2n+1} - r^{2n+1}) + b_8 (R^{2n+2} - r^{2n+2}) \end{array} \right] \quad (35)$$

$$v_p = v_s - 2 \tau_y [a(t)]^{n-1} (R^n - R_{0p}^n) + \frac{2[a(t)]^n}{(n+1)} (R^{n+1} - R_{0p}^{n+1}) + \alpha^2 \left[ \begin{array}{l} 2b_2 (R^n - R_{0p}^n) - b_3 (R^{2n} - R_{0p}^{2n}) \\ + b_4 (R^{2n+1} - R_{0p}^{2n+1}) + 2b_6 (R^{n+1} - R_{0p}^{n+1}) \\ - 2b_7 (R^{2n+1} - R_{0p}^{2n+1}) + b_8 (R^{2n+2} - R_{0p}^{2n+2}) \end{array} \right] \quad (36)$$

With the help of equation (25) and (31) in (18), the shear stress  $\tau$  can be obtained as

$$\tau = (\tau_0 + \alpha^2 \tau_1)_{r=R} \quad (37)$$

$$\tau = [ra(t) + \alpha^2 \{a_5 r - a_4 r^{n+1} + a_6 r^{n+2}\}]_{r=R}$$

The volumetric flow rate Q can be calculated, with the help of equation (15) and expression of velocity and obtained as

$$Q = 2R^2 v_s - 4q_2 R^{n+2} + 4q_3 R^{n+3} + 4\alpha^2 q_4 R^{n+2} - 2\alpha^2 q_5 R^{2n+2} + 2\alpha^2 q_6 R^{2n+3} + 4\alpha^2 q_7 R^{n+3} - 4\alpha^2 q_8 R^{2n+3} + 2\alpha^2 q_9 R^{2n+4} \quad (38)$$

Where

$$q_1 = n[a(t)]^{n-1}, q_2 = q_1 / (n+2), q_3 = a(t)q_1 / n(n+3), q_4 = nb_2 / (n+2), q_5 = nb_3 / (n+1)$$

$$q_6 = 2n(1-n)b_1 a_6 / (2n+3), q_7 = q_1 a_5 / (n+3), q_8 = q_1 a_4 / (2n+3), q_9 = q_1 a_6 / (n+2),$$

The second approximation plug core radius  $R_{1p}$  can be obtained by neglecting terms of  $\alpha^4$  and higher powers of  $\alpha$  in the following manner in equation (19). The shear stress at  $r = R_p$  is given by

$$\tau_y = (\tau_0 + \alpha^2 \tau_1)_{r=R_p} \quad (39)$$

Equation (39) shows the fact that on the boundary of the plug core region the existing value of shear stress and yield stress are same. The plug core radius  $R_{1p}$  can be obtained by using the Taylor's series of  $\tau_0$  and  $\tau_1$  about  $R_{0p}$  and using

$$\tau_0 = \tau_y \text{ at } r = R_{0p} \text{ as}$$

$$R_{1p} = \frac{\tau_1(R_{0p})}{a(t)} \quad (40)$$

With the help of equation (24) and (32) in (21), the shear stress  $\tau_p$  can be obtained as

$$\tau_p = R_{0p} a(t) + \alpha^2 \{a'_5 R_{0p} - a'_4 R_{0p}^{n+1} + a'_6 R_{0p}^{n+2}\} \quad (41)$$

With the help of equation (19), (30), (32) and (40), the plug core radius  $R_p$  can be obtained as

$$R_p = R_{0p} + \frac{\alpha^2}{a(t)} \{a'_5 R_{0p} - a'_4 R_{0p}^{n+1} + a'_6 R_{0p}^{n+2}\} \quad (42)$$

The effective viscosity in the non-dimensional form is given by

$$\mu_e = \frac{(R(z))^4}{Q(z,t)} (1 + e \cos t)$$

$$\mu_e = (R(z))^2 (1 + e \cos t) \{ 2v_s - 4q_2R^n + 4q_3R^{n+1} + 4\alpha^2q_4R^n - 2\alpha^2q_5R^{2n} + 2\alpha^2q_6R^{2n+1} + 4\alpha^2q_7R^{n+1} - 4\alpha^2q_8R^{2n+1} + 2\alpha^2q_9R^{2n+2} \}^{-1} \tag{43}$$

**4. RESULTS AND DISCUSSION**

In this analysis the expression of axial velocity, flow rate, wall shear stress and effective viscosity are obtained and computed for the fixed values of  $F = 0.2$ ,  $n = 0.95$ ,  $m = 2$ ,  $\varphi = 0.2$ ,  $\tau_y = 0.1$ ,  $\omega = 1$  [7, 10, 24]. Fig.2 - Fig.7 reveals the variation of axial velocity with radial distance and depicts that the axial velocity is maximum at  $r = 0$  and decreases with the increase in the radius of artery  $r$  and attains minimum value near the stenotic wall at  $r = R(z)$ . Hence the fluid velocity decreases as the radial distance increases. Fig.2 - Fig.4 depicted that the fluid velocity augmented with the increase in slip velocity, Body acceleration and pressure gradient.

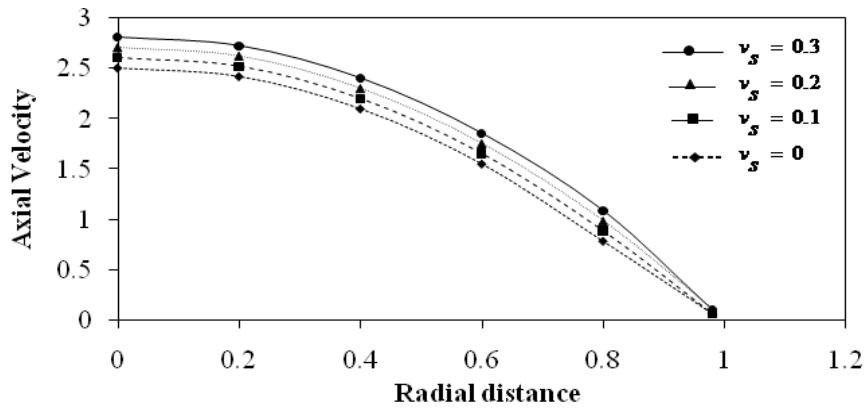


Fig. 2. Variation of axial velocity with the radial distance for different values of slip velocity with  $B = 1$ ,  $\alpha = 0.1$ ,  $e = 1$ ,  $\delta = 0.1$ .

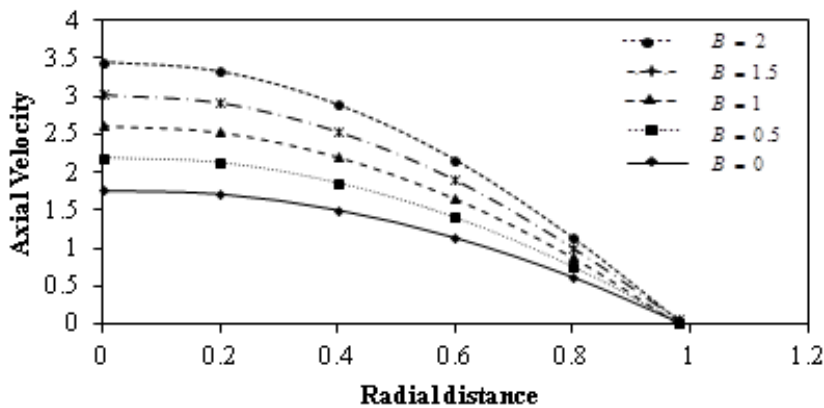


Fig. 3. Variation of axial velocity with the radial distance for different values of body acceleration parameter with  $\alpha = 0.1$ ,  $e = 1$ ,  $\delta = 0.1$ .

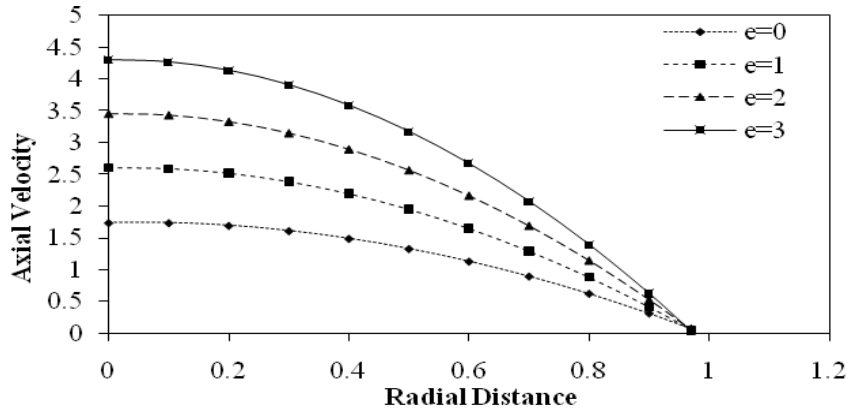


Fig. 4. Variation of axial velocity with the radial distance for different values of pressure gradient parameter with  $B = 1, \alpha = 0.1, v_s = 0.1, \delta = 0.1$ .

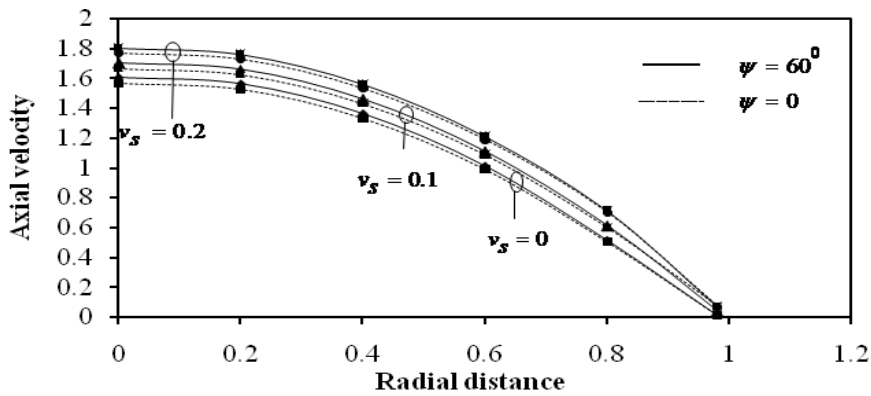


Fig. 5. Variation of axial velocity with the radial distance for different values of slip velocity and inclination angle with  $B = 1, \alpha = 0.1, t = 1, \delta = 0.1$ .

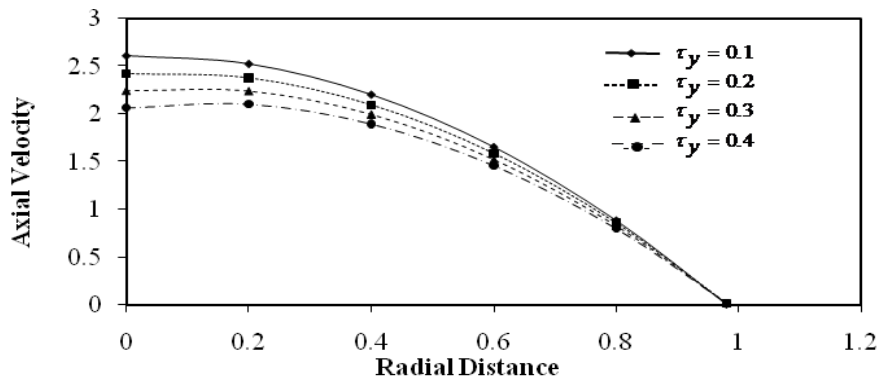


Fig.6. Variation of axial velocity with the radial distance for different values of yield stress with  $B = 1, \alpha = 0.1, e = 1, \delta = 0.1$ .

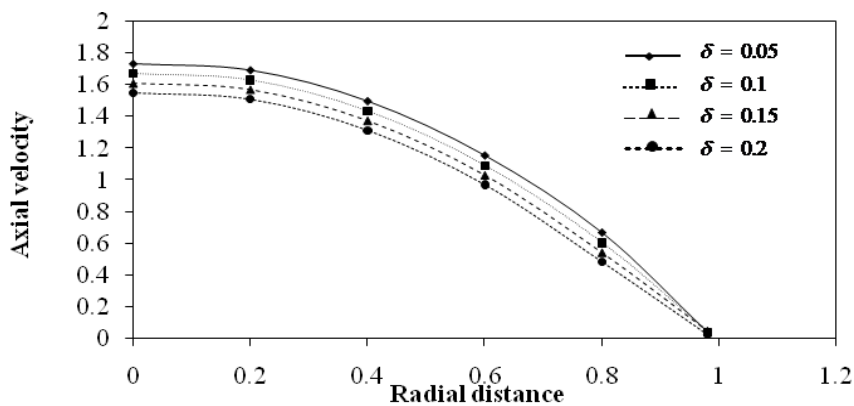


Fig.7. Variation of axial velocity with the radial distance for different values of stenosis height with  $B = 1, \alpha = 0.1, v_s = 0.1, e = 1$ .



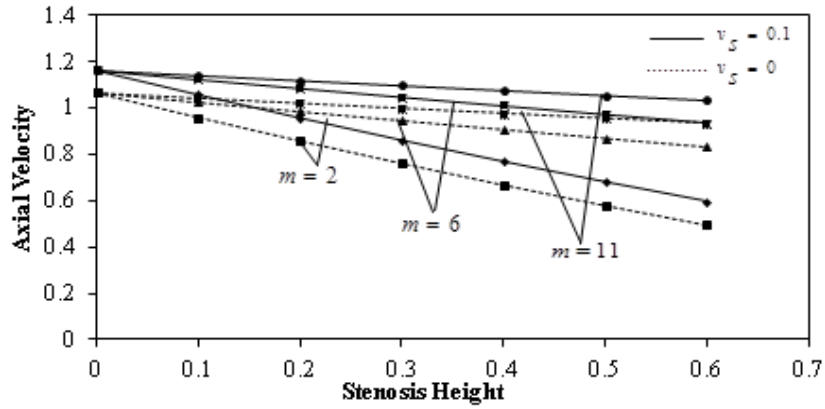


Fig. 8. Variation of axial velocity with the stenosis height for different shape parameters and slip velocity with  $B = 1, \alpha = 0.1, e = 0$ .

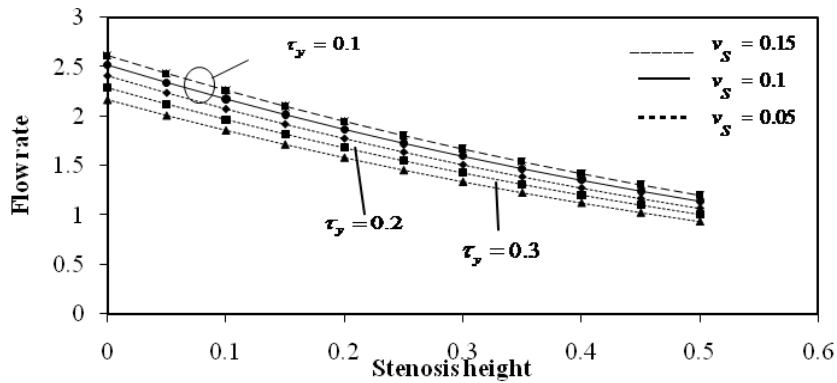


Fig. 9 . Variation of axial velocity with the radial distance for different values of slip velocity and yield stress with  $B = 1, \alpha = 0.1, t = 1, e = 1$ .

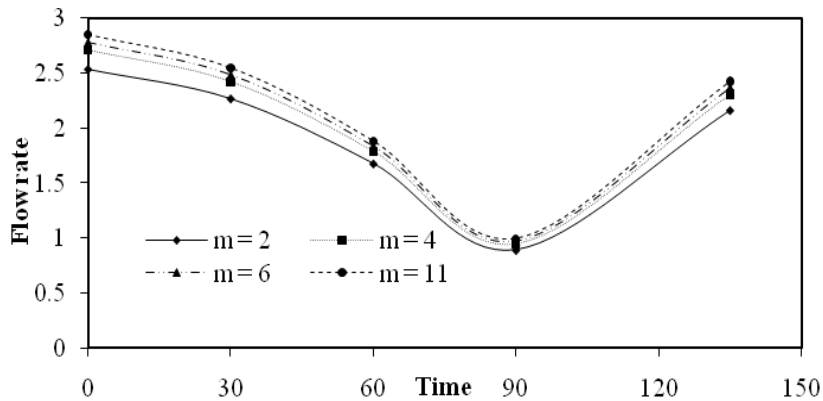


Fig. 10 . Variation of flow rate with time for different values of shape parameter with  $B = 1, \alpha = 0.1, t = 1, \delta = 0.1$ .

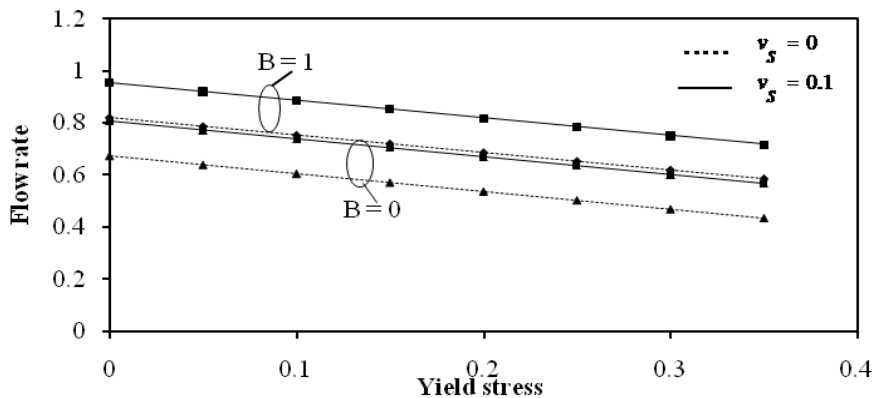


Fig. 11. Variation of flow rate with yield stress for different values of body acceleration and slip with  $\alpha = 0.1, \delta = 0.5, e = 1$ .

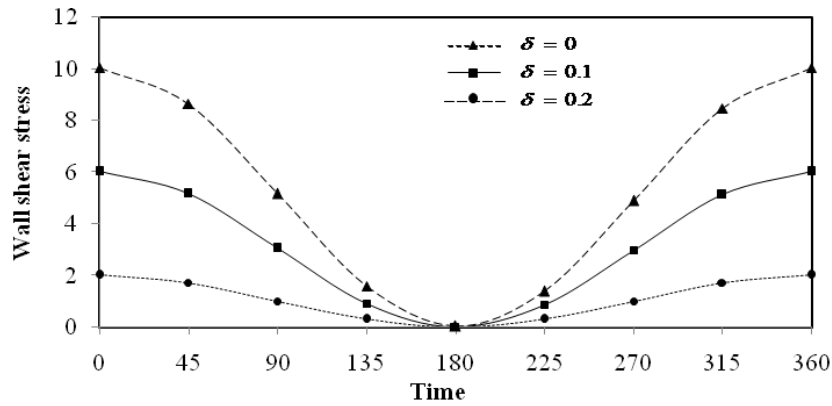


Fig. 12. Variation of wall shear stress with time for different values of stenosis shape parameter with  $B = 0, \alpha = 0.5, L = 2, e = 1$ .

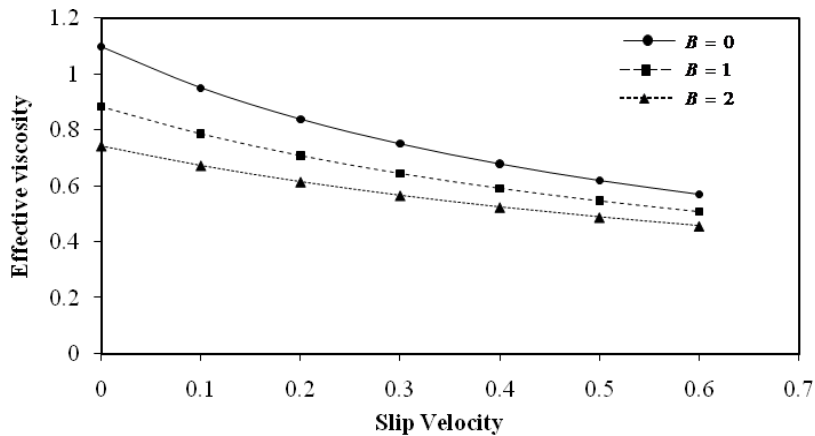


Fig. 13. Variation of effective viscosity with the slip velocity for different values of body acceleration with  $e = 1, \alpha = 0.1, t = 1, \delta = 0.1$ .

Fig.5 shows that the magnitude of velocity increases in inclined artery along with the increase in slip as compared to the non inclined artery while Fig.6 - Fig.7 shows that it decreases with the increase in yield stress or stenosis height. The variation of axial velocity with the stenosis height for different values of shape parameter and slip is shown in Fig.8 and it demonstrated that the axial velocity of blood slightly increases with increase in shape parameter and slip. This proposes that velocity of blood increases as stenosis loses its symmetry. Fig.9 illustrates that the flow rate decreases with the increase in yield stress and stenosis height but in the presence of slip velocity flow rate moderately increases. In Fig.10 the effect of stenosis shape parameter has been observed for flow rate versus change in time and we observed that the flow rate augmented when stenosis loses its symmetry ( $m = 2$ ), i. e. for larger value of shape parameter. It is also noticed that flow rate is maximum at  $t = 0$  and then starts decreasing from 0 to  $90^\circ$  along the time and attains minimum value at  $t = 90^\circ$ , then again it starts increasing for maximum value. Fig.11 consists of the variation of flow rate with the yield stress and it shows that the flow rate increases with the increase in body acceleration and slip velocity while increase in yield stress results a substantial decrease in flow rate. This decrease in flow rate is due to increase in the width of plug flow region. The variation of wall shear stress with time for different values of stenosis height is shown in Fig.12. It is observed from the figure that the wall shear stress gradually decreases as time increases and it attains the symmetry about  $t = 180^\circ$ . Fig.13 describes the effect of body acceleration on effective viscosity versus slip velocity and it depicts that the effective viscosity decreases with the increase in Body acceleration along with the increment in slip velocity.

## 5. CONCLUSION

Present model has been developed on pulsatile blood flow through an inclined stenosed artery with periodic body acceleration and axial slip velocity at the constricted wall along with the effect of stenosis shape parameter. The body fluid flow is assumed to behave like a non-Newtonian fluid and represented a Herschel bulkely fluid model. Analytic expressions for flow variables and their variations with different flow parameters have been obtained and are represented graphically. The results based on the mathematical analysis and the subsequent numerical evaluation of the flow quantities indicates that the axial velocity and flow rate increases with the increase in body acceleration, inclination angle, pressure gradient and slip velocity while decreases with the increase in yield stress and stenosis height. Wall shear stress gradually decreases as time increases and it attains the symmetry about  $t = 180^\circ$ . Effective viscosity decreases with the increase in body acceleration and slip. This model concludes that slip velocity play a very significant role in blood flow modeling in an inclined stenosed artery. It has been observed that the axial velocity and

flow rate decreases with the increase in yield stress and stenosis height. It may also be concluded that damages to the vessel wall could be reduced with the help of slip. So this study may help the physicians in estimating the severity of stenosis and its consequences in future or for the treatment of cardiovascular diseases like myocardial infarction, cerebral accident, heart attacks etc. This study may further extend by the introduction of more rheological and physical parameters in the case of more severe stenosis.

## 6. REFERENCES

1. C. Tu, M. Deville, Pulsatile flow of non-Newtonian fluids through arterial stenosis. *J Biomech.* 29 (1996), 899–908.
2. D. Biswas, *Blood flow models: A comparative study*, Mittal Publications, New Delhi, India, (2000).
3. D. Biswas and M. Paul, Study of blood flow inside an inclined non-uniform stenosed artery, *International Journal of Mathematical Archive* 4(2013), 33-42.
4. D.C. Sanyal, K. Das and S. Debnath, Effect of magnetic field on pulsatile blood flow through an inclined circular tube with periodic body acceleration, *Journal of Physical Sciences* 11(2007), 43-56.
5. D. F Young, Effects of time dependent stenosis on flow through a tube. *J. Eng Ind Trans ASME* 90(1968), 248–54.
6. D. F Young, Fluid mechanics of arterial stenosis, *J. Biomech Eng. (Trans ASME)* 101(1979), 157–75.
7. D. F Young, F.Y Tsai, Flow characteristics in models of arterial stenosis – I. Steady flow. *J Biomech.* 6 (1973), 395–411.
8. D. S Sankar, Usik Lee, Mathematical modeling of pulsatile flow of non-Newtonian fluid in stenosed arteries, *Commun Nonlinear Sci Numer Simul.* 14(2009), 2971–2981.
9. D. S. Sankar and K. Hemalatha, — Pulsatile flow of Herschel-Bulkley fluid through stenosed arteries—a mathematical model, *I. J. of Non-Linear mechanics* 41-8 (2006), 979–990.
10. D. W. Lipsch, Flow in tubes and arteries – a comparison. *Biorheology* 23(1986), 395–433.
11. G. Neeraja, K. Vidya, Effect of body acceleration on pulsatile flow of Herschel –Bulkley fluid through an inclined mild stenosed artery, *IJERT Issue-5, 1(2012)*, ISSN: 2278-0181.
12. G.T. Liu, X.J. Wang, B.Q. Ai, L.G. Liu, Numerical study of pulsating flow through a tapered artery with stenosis, *Chin. J. Phys.* 42(2004), 401–409.
13. H. Schlichting, K. Gersten, *Boundary layer theory*, Springer-Verlag, 2004.
14. J. C Mishra, M. K Patra, S.C Mishra, A non-Newtonian fluid model for blood flow through arteries under stenotic conditions. *J Biomech.* 26(1993), 1129–41.
15. J. N. Kapur *Mathematical models in biology and medicine*. New Delhi, India: Affiliated East-West Press Pvt. Ltd. (1992), 368-69.
16. K. Maruti Prasad and G. Radhakrishnamacharya, Flow of Herschel-Bulkley fluid through an inclined tube of non-uniform cross section with multiple stenosis, *Arch. Mech.* 60(2008), 161-172.
17. K. Vajravelu, S. Sreenadh, V. Ramesh Babu, Peristaltic transport of a Herschel Bulkley fluid in an inclined tube, *Int. J. of Non-Linear Mech.* 40 (2005), 83-90, <http://dx.doi.org/10.1016/j.ijnonlinmec.2004.07.001>
18. M.K. Sharma, K. Singh and S. Bansal, Pulsatile MHD flow in an inclined catheterized stenosed artery with slip on the wall, *J. Biomedical Science and Engineering*, 7 (2014), 194-207. <http://dx.doi.org/10.4236/jbise.2014.74023>
19. N. Iida, Influence of plasma layer on steady blood flow in micro vessels, *J. A. Phy.* 17(1978), 203–214.
20. P. Chaturani and D. Biswas, Effects of slip in flow through stenosed tube, *Physiological Fluid Dynamics, Proc. of 1<sup>st</sup> International Conference on Physiological Fluid Dynamics* (1984), 75-80.
21. P. Chaturani, R. Ponnalagar Samy, Pulsatile flow of Casson's fluid through stenosed arteries with applications to blood flow, *Biorheology* 23(1986), 499–511.
22. P. Chaturani, V.S. Upadhyaya, Gravity flow of fluid with couple stress along an inclined plane with application to blood flow, *Journal of Biorheology* 14 (1977), 237-246.
23. S. Chakravarthy, P. K. Mandal, Two-dimensional blood flow through tapered arteries under stenotic conditions, *Int. J. Non-Linear Mech.* 35(2000), 779–793.
24. S. Ookawara, K. Ogowa, Flow properties of Newtonian and non-Newtonian fluid downstream of stenosis, *J. Chem. Eng. Japan* 33(2000), 582–90.
25. S. R. Shah, An innovative solution for the problem of blood flow through stenosed artery using generalized bingham plastic fluid model, *IJRANSS*, 1(3) (2013), 97-104.
26. S.U Siddiqui, N. K Verma, S. Mishra, R. S. Gupta, Mathematical modeling of pulsatile flow of Casson fluid in arterial stenosis. *Appl Math Comput.*, 210, Issue-1(2009), 1-10, [doi.org/ 10.1016/j.amc.2007.05.070](http://dx.doi.org/10.1016/j.amc.2007.05.070).
27. V.K. Sud, G.S. Sekhon, Arterial flow under periodic body acceleration. *Bulletin of Mathematical Biology*. 47 (1985) 35-52.

**Source of support: Nil, Conflict of interest: None Declared.**

**[Copy right © 2017. This is an Open Access article distributed under the terms of the International Journal of Mathematical Archive (IJMA), which permits unrestricted use, distribution, and reproduction in any medium, provided the original work is properly cited.]**